Taylor & Francis
Taylor & Francis Group

ORIGINAL RESEARCH

🔓 OPEN ACCESS   Check for updates

Lactate/GPR81 recruits regulatory T cells by modulating CX3CL1 to promote immune resistance in a highly glycolytic gastric cancer

Jin Su[a,b], Xinyuan Mao[a], Lingzhi Wang[a], Zhian Chen[a], Weisheng Wang[a], Cuiyin Zhao[a], Guoxin Li[a], Weihong Guo[a], and Yanfeng Hu [iD][a]

[a]Department of General Surgery & Guangdong Provincial Key Laboratory of Precision Medicine for Gastrointestinal Tumor, Nanfang Hospital, The First School of Clinical Medicine, Southern Medical University, Guangzhou, China; [b]Department of General Surgery, Zhuzhou Hospital affiliated to Xiangya School of Medicine, Central South University, Zhuzhou, China

ABSTRACT

Lactate plays an important role in shaping immune tolerance in tumor microenvironment (TME) and correlates with poor prognosis in various solid tumors. Overcoming the immune resistance in an acidic TME may improve the anti-tumor immunity. Here, this study elucidated that via G-protein-coupled receptor 81 (GPR81), lactate could modulate immune tolerance in TME by recruiting regulatory T cells (Tregs) in vitro and in vivo. A high concentration of lactate was detected in cell supernatant and tissues of gastric cancer (GC), which was modulated by lactic dehydrogenase A (LDHA). GPR81 was the natural receptor of lactate and was overexpressed in different GC cell lines and samples, which correlated with poor outcomes in GC patients. Lactate/GPR81 signaling could promote the infiltration of Tregs into TME by inducing the expression of chemokine CX3CL1. GPR81 deficiency could decrease the infiltration of Tregs into TME, thereby inhibiting GC progression by weakening the inhibition of CD8$^+$T cell function in a humanized mouse model. In conclusion, targeting the lactate/GPR81 signaling may potentially serve as a critical process to overcome immune resistance in highly glycolytic GC.

Introduction

Lactate in the tumor microenvironment (TME) is the product of glycolysis and is emerging as a pivotal modulator of tumor growth, metastasis, and anti-tumor immunity.[1–3] Known as metabolic waste previously, lactate is now considered a universal fuel to feed tumor cells and tumor stromal cells.[4] Lactate secreted from tumor cells may lead to immunosuppression either by inhibiting the proliferation and activation of CD8$^+$T cells, antigen-presenting cells, natural killer cells, or potentiating the immunosuppressive effect of regulatory T cells (Tregs) and polarization of macrophage to M2-like phenotype.[5–8] Recently, increasingly more attention has been paid to GPR81, a lactate natural receptor, which is correlated with tumor cell survival, ferroptosis, and immune evasion.[9–12] So far, it remains unclear regarding the specific mechanism by which lactate induces immune escape in gastric cancer (GC).

According to previous research on the immune landscape in GC and esophageal squamous cell carcinoma, the immunosuppressive micro-environment enriched with exhausted T cells, NK cells, Tregs, tumor-related macrophage, and tolerogenic dendritic cells, among which Tregs are the dominant ones.[13,14] Moreover, some patients do not respond or develop immune suppression during immunotherapy in real-world clinical scenarios.[15,16] There is increasing evidence that Tregs can attenuate the effects of immunotherapy.[17–19] Tregs can suppress the lethality of effector T cells to tumor cells, and

correlate with tumor progression and poor prognosis.[20] Thus, decreasing the infiltration of Tregs into TME may potentially recover the anti-tumor immune response and enhance the effects of immunotherapy.

Chemokines in TME are the primary motivators for Tregs infiltration. The reported chemokines that modulate Tregs migration in tumors include C-C motif ligand (CCL) 1, CCL5, CCL20, CCL22, CCL28, and chemokine C-X-C motif ligand 12 (CXCL12).[21,22] Blocking chemotaxis signal transduction can decrease the accumulation of Tregs in TME, and then suppress tumor progression in various solid tumors.[23–26] Nevertheless, it is still unknown regarding the dominant chemokine type to drives the infiltration of Tregs in an acidic GC micro-environment. Therefore, it is of great significance to clarify the relationship between the immune escape aroused by GC cell-derived lactate and the infiltration of Tregs in the tumor microenvironment.

Materials and methods

Blood and GC samples

The healthy human peripheral blood was donated by the members of our Laboratory, and each member was fully informed that the sampling was to acquire peripheral blood mononuclear cells (PBMCs) and sort Tregs. Two cohorts of human GC samples were collected and used in the study, with

written informed consent obtained from all subjects. Cohort 1 included 31 GC tumor tissues and corresponding 24 adjacent normal tissues collected from GC patients who underwent radical gastrectomy from July 2021 to June 2022 at the Department of General Surgery of Nanfang Hospital, Southern Medical University. The tumor and normal tissues were immersed in RNA Stabilization and Storage solution (Thermo Fisher, USA) after being washed by PBS postoperatively and stored in liquid nitrogen. Cohort 2 contained 20 pairs of paraffin-embedded GC tumors and normal tissues collected from patients who underwent surgery from June to December 2020 at the same Department of the hospital. This study was approved by the Institutional Ethics Committee of Nanfang Hospital, Southern Medical University.

Cell lines and cell culture

The human GC cell lines AGS, HGC-27, MKN-28, SNU-216, MGC-803, BGC-823, SGC-7901, human colon cancer cell line HCT-116, human breast cancer cell line MCF-7, and human normal gastric epithelial cell line GES-1 were obtained from American Type Culture Collection (ATCC, USA). All cells were cultured in RPMI1640 (Gibco, C11875500BT) supplemented with 10% fetal bovine serum (FBS; Gibco, A3160902) and 1% penicillin-streptomycin (Gibco 15,140,122) in a humidified incubator at 37°C with 5% CO_2.

RNA extraction and RT-qPCR

Total RNA was extracted and purified from GC cell lines and tissues with Trizol reagent (Invitrogen, USA) according to the manufacturer's protocols. The concentration of the total RNA was examined by NanoDrop 2000 (Thermo Fisher, USA). cDNA was synthesized using the Evo M-MLV RT Premix (Accurate Biology, AG11706). The primers used in the study were listed in Supplementary Table 1. qPCR was performed by using SYBR Green Pro Taq Hs qPCR Kit (Accurate Biology, AG11701). GAPDH or β-actin was used to normalize the difference between groups.

Western blot analysis

Proteins were extracted from GC cell lines using RIPA lysis buffer (Thermo Fisher, USA) supplemented with 1% protease and phosphatase inhibitors (Thermo Fisher, USA), and incubated for 30 min on ice. The concentration of the collected protein was detected by bicinchoninic acid (BCA) Protein Assay Reagent (Beyotime, P0009). A total of 20 μg protein of each sample was added and separated by sodium dodecyl sulfate–polyacrylamide gel electrophoresis (SDS-PAGE). The target proteins were transferred to polyvinylidene difluoride (PVDF) membranes (Millipore, GVWP04700). An enhanced chemiluminescent kit HRP (Fdbio, FD8000) was used for image development. The gray value of the protein band was measured by Image J software (National Institutes of Health, USA). Antibodies used in the study were anti-Tubulin (1:1000 dilution, Abmart, M20005), anti-FOXP3 (1:1000 dilution, Bioss, bsm-52,079 R), anti-GPR81 (1:500 dilution, Novus, NLS2095), anti-CX3CL1 (1:1000 dilution, Bioss, bs-0811 R), anti-p65 (1:1000 dilution, Abmart, T55034), anti-phospho-p65 (1:1000 dilution, Abmart, TA2006), and anti-LDHA (1:1000 dilution, Abcam, ab101562).

Immunohistochemistry (IHC) and immunofluorescence

IHC was performed by using paraffin-embedded human GC tissues and mouse-bearing tumors. Sections were incubated with anti-GPR81 (1:100 dilution), anti-LDHA (1:200 dilution), anti-CX3CL1 (1:100 dilution), anti-FOXP3 (1:100 dilution), and anti-phospho-p65 (1:100 dilution) at 4°C overnight. Another incubation was conducted with an anti-rabbit secondary antibody (1:200 dilution). The stained image was analyzed by Image J software. The staining intensity of the tissue slides was assessed as described previously.[27]

Immunofluorescence was performed after GC cells were seeded on the slides and cultured for 24 h. Cells were incubated with anti-GPR81 (1:50 dilution), anti-CX3CL1 (1:100 dilution), and anti-p65 (1:100 dilution) overnight at 4°C. Immunofluorescence images were obtained by fluorescence microscope (Zeiss, Germany).

siRNA and plasmids transfection

Small interfering RNA (siRNA), plasmids containing small hairpin RNA (shRNA), and overexpression plasmids were obtained from Tsingke Biotech (Beijing, China) and were transfected into GC cell lines to knock down or overexpress the target gene. siNC, shNC, and oeNC were used as the negative control separately. The sequence was listed in Supplementary Table 2. The decreased expression of the target gene was confirmed by RT-qPCR and western blot.

Cell viability assay

The proliferation rate of GC cells after GPR81 knockdown or overexpression and the cytotoxicity of $CD8^+T$ cells to GC cells were assessed using the CCK8 kit (Dojindo, DK4) according to the manufacturer's instructions. GC cells were seeded onto the 96-well plate at a density of 3,000 cells per well, and cultured in RPMI1640 containing 10% FBS in a 37°C incubator with 5% CO_2. The $CD8^+T$ cells co-cultured with GC cells at the ratio of 20:1 with or without lactate (20 mmol/L), and cultured for 48 h. PBS was washed twice before detection. Cell viability was detected by measuring the absorption at the wavelength of 450 nm with a plate reader (Molecular Devices, USA).

Lactate assay

The detection of lactate in GC cell line-cultured supernatants (48 h) and GC samples was performed according to the manufacturer's protocols of the L-Lactate Content Test Kit (Solarbio, BC2230). For lactate detection in tissues, specifically, weighing 0.1 g of tissue was added in reagent one for adequate homogenization. The next step was centrifugation at 4°C and 12,000 g for 10 min to obtain the supernatant for the lactate test. The content of the detected lactate was shown as μmol/g.

Enzyme-linked immunosorbent assay (ELISA)

The concentration of CX3CL1 in the supernatant of GC cell lines under different interference was detected by the CX3CL1 ELISA kit (Solarbio, SEKH0067) according to the manufacturer's protocols.

Dual-luciferase reporter assay

GC cells were seeded onto a 96-well plate at the concentration of 3,000 cells per well for 24 h of culture. The cells were transfected with CX3CL1 promoter sequence plasmids (Genechem, Shanghai, China) persistently expressing firefly luciferase. The pRL-TK plasmids persistently expressing Renilla luciferase (the control) were used to evaluate the transfection efficiency. A dual luciferase reporter gene kit (Beyotime, China) and a multifunctional enzyme labeling instrument (Molecular Devices, USA) were used to detect the luciferase activity of each group.

Isolation of Tregs and Tconv, and generation of induced Tregs (iTregs)

Fluorescence-activated cell sorter (FACS) was used to isolate Tregs and Tconv from healthy donors' PBMCs. PBMCs were resuspended in 100 μl PBS and stained with CD4 (10^6 cells per test) (Bioscience 555,348), CD25 (10^6 cells per test) (Bioscience 555,434), and CD127 (10^6 cells per test) (Bioscience 557,938) monoclonal antibodies for 20–30 min on the ice in dark. $CD4^+CD25^+CD127^-$ cells were identified as Tregs,[28] and $CD4^+CD25^-$ cells were known as naive conventional T (Tconv) cells.

iTregs generation and differentiation were induced by following the protocols published previously.[29] In short, the sorted Tconv cells were seeded onto 24-well plates which were pre-coated with 1 μg/ml anti-CD3 (Biolegend 317,325) overnight. The cells were cultured in RPMI1640 containing 10% FBS and were supplemented with 1 μg/ml anti-CD28 (Biolegend 302,933), 5 ng/ml TGF-β1 (Peprotech, 100–21), and 20 ng/ml IL2 (Novoprotein, C013) for 3 days. Then, cells were washed with PBS and cultured in a complete RPMI1640 medium supplemented with 20 ng/ml IL2 for 4 to 7 days. The harvested cells were collected for further studies and verification of the suppressive effect on $CD8^+T$ cells.

Chemotaxis assay

iTregs (2×10^5) were induced from Tconv which were sorted from healthy donator's PBMCs, and then resuspended by PBS and transferred into the upper chamber (8 μm-pore size) of the Transwell system (Corning, USA). Recombinant human CX3CL1 was diluted by RPMI1640 with different concentrations (0, 10 pg/ml, 100 pg/ml, 1 ng/ml, 10 ng/ml, and 100 ng/ml) and added into the lower chamber with a total volume of 600 μl. The migrated cells in the lower chamber were counted after culture at 37°C for 6 h in a 5% CO_2 atmosphere. For detecting migration, PBMCs (1×10^6) separated from healthy donors' peripheral blood were inoculated into the upper chamber (total volume of 100 μl). Conditional supernatants (GPR81 knockdown or overexpression, p65 knockdown, CX3CL1 knockdown or CX3CL1 solution) of GC cell lines (total volume of 600 μl) were transferred into the lower chamber. The ratio of Tregs and $CD8^+T$ cells in PBMCs collected from the lower chamber was analyzed by flow cytometry after co-culture for 6 h.

FACS analysis

Cells from the lower chamber were collected and resuspended in 100 μl PBS to detect the ratio of Tregs and $CD8^+T$ cells in migrated PBMCs after Transwell assay. The cells were stained with CD4 (10^6 cells per test), CD8 (10^6 cells per test, Bioscience 560,662), CD25 (10^6 cells per test), and CD127 (10^6 cells per test) monoclonal antibodies for 20–30 min on ice in dark. The test was performed after two times of centrifugation. The gate setting followed the manufacturer's protocols. To test the blood sample taken from the posterior orbital venous plexus of M-NSG mice before PBMCs injection, mouse-derived antibodies CD3 (10^6 cells per test, Bioscience 740,147), CD45 (10^6 cells per test, Bioscience 557,659), and CD4 (10^6 cells per test, Bioscience 553,047) were used.

This experiment also detected the ratio of Tregs and $CD8^+T$ cells in subcutaneous tumors of the humanized mouse model. Single-cell suspension was prepared by adding 50 μg/ml DNase I (Stemcell, 100–0683 07470 07469) and 1 mg/ml collagenase type IV (Stemcell 07,909) to dissolve tumor tissues. Red blood cell lysis buffer (Fdbio, FD7153) was used to eliminate red blood cells. The cells were stained with CD3 (10^6 cells per test, Bioscience 564,713), CD45 (10^6 cells per test, Bioscience 557,833), CD4 (10^6 cells per test), CD8 (10^6 cells per test), CD25 (10^6 cells per test), and CD127 (10^6 cells per test) monoclonal antibodies. Fluorescence data acquired from FACS were analyzed by Flow Jo software (BD, USA).

Humanized xenograft mouse model

A tumor-bearing humanized mouse model was constructed following the method reported previously.[30] The tumor cells (5×10^6) transfected with lentiviral (Lv) particles (GeneCopoeia, Shanghai, China) containing GPR81 shRNA were injected into the subcutaneous area in the right low flank of the NOD.Cg-Prkdc^{scid}IL2rg^{em1Smoc} (M-NSG) male mice (8 to 12 weeks, Shanghai Model Organisms Center, Inc., China). After 5 to 7 days of tumor inoculation, 1×10^7 PBMCs were injected through the tail vein to reconstruct the immune system. Blood was drawn from the posterior orbital venous plexus to detect the immune cells after 3 weeks of PBMC administration. Tumor volume was measured by using a vernier caliper every 4 days and calculated according to the formula: Volume (V) = (L×S^2)/2 mm^3, where L is the long diameter and S is the short diameter of the tumor. Endpoints were either 4 weeks after immune reconstitution or after tumor volume reached 1500 mm^3. The study was approved by the Animal Care and Use Committee of Southern Medical University and all procedures performed followed the guidance of the Laboratory Animal Center.

Statistics

Data in the study were shown as mean±standard deviation (SD) or mean±standard error of the mean (SEM). Statistical analysis was performed in GraphPad Prism (USA). For continuous parameters, statistical significance between groups was calculated by unpaired Student t-test. For categorical variables, statistical difference comparison was analyzed by the Chi-square test. The comparison of variables among multiple groups was realized by using one-way analysis of variance (ANOVA). P-value <.05 was considered to indicate a statistically significant difference.

Results

GC was a highly glycolytic tumor with a high concentration of lactate

To explore the expression of LDHA in GC, we initially evaluated the LDHA mRNA level and protein expression in primary GC tissues and adjacent normal tissues (Figure 1(a,b)). There were differences in expression (high, moderate, and low) among different samples (tumor and normal). LDHA expression in GC tissues was significantly higher than that in adjacent normal tissues. We further explored LDHA expression in six GC cell lines by RT-qPCR (Figure 1(c)) and Western blot (Figure 1(d)) in vitro. Consequently, high expression of LDHA was found in some GC cell lines. Moreover, the concentration of lactate in most culture supernatant of GC cells was higher than that in GES-1 (Figure 1(e)). The same results were found in the GC samples(Figure 1(f)). These data indicated that GC was a highly glycolytic tumor and could produce abundant lactate to create an acidic TME.

GPR81 was overexpressed in GC and positively correlated with the Tregs infiltration

To explore the expression level of GPR81 in GC, human GC samples were collected for RT-qPCR and IHC (Figure 2(a, b)). The results showed that GPR81 was overexpressed in GC tissues. Furthermore, data from The Cancer Genome Atlas Program (TCGA) exhibited that GPR81 expression correlated with the overall survival in GC (Figure 2(c)). We verified the results via in vitro experiment, according to the comparison between GC cells and GES-1, GPR81 mRNA and protein levels were both higher in some GC cell lines (Figure 2(d,e)).

This study further clarified whether tumor infiltration of Tregs correlated with GPR81 expression levels. Data from TCGA (www.camoip.net) suggested that GPR81 expression in GC tissues had a significant positive correlation with tumor infiltration of Tregs (Figure 2(f)). We then verified the results in human GC samples. As expected, the expression of FOXP3 (a unique marker of Tregs) levels showed a positive correlation with GPR81 expression (Figure 2(g,h)). Altogether, these data illustrated that GPR81 was highly expressed in GC tissues and cells, and correlated with GC overall survival or tumor infiltration of Tregs.

Lactate/GPR81 modulated the expression of CX3CL1 in GC cells

To assess the possible immunomodulatory role of lactate signaling in GC, we sought to discover the correlation between lactate signaling and chemokines expressed in GC cells. As shown in Figure 3(a), SGC-7901 incubated with lactate exhibited high expressions of multiple chemokines. Among the explored chemokines, CX3CL1 was significantly upregulated after being stimulated by lactate. Of note, CX3CL1 mRNA expression levels significantly correlated with GPR81 mRNA expression levels in human GC samples (Figure 3(b)). RT-qPCR and Western blot were then conducted to detect CX3CL1 expression levels in GC cell lines after incubation with lactate at different time points. The strongest CX3CL1 expression was observed at 6 h after being stimulated with lactate (Figure S1A-1B). Surprisingly, the CX3CL1 expression level gradually upregulated with the increase of lactate concentration in GC cell lines (Figure 3(c, d)). We further explored that lactate upregulated CX3CL1 expression in human colon cancer cell HCT-116 and breast cancer cell MCF-7, and this correlation was dependent on lactate concentration (Figure S1C).

We further explored whether the aforementioned biological effects of lactate relied on its receptor GPR81. Downregulation of CX3CL1 expression was observed when GPR81 was knockdown compared with that after transfection of empty vector in SNU-216 (Figure 3(e)). ELISA of GC cell culture supernatant suggested that the concentration of CX3CL1 decreased when GPR81 was knocked down (Figure 3(f)). Moreover, the expression of CX3CL1 maintained low levels with the gradually increased concentrations of lactate after interfered with GRP81 shRNA. (Figure 3(g)). Plate cloning assay and CCK8 assay were employed to test the proliferation of GC cells. Interestingly, the proliferation of GC cells showed no significant difference after knockdown or overexpression of GPR81 when compared with the wild type (Figure S1D-1E). Collectively, these data suggested that lactate could modulate CX3CL1 expression through GPR81 in GC cell lines.

Lactate/GPR81 recruited Tregs by modulating CX3CL1 expression

We next examined whether lactate/GPR81 recruited Tregs migration in vitro via CX3CL1. Firstly, we sorted and purified Tconv (CD4$^+$CD25$^-$ T cells) and Treg (CD4$^+$CD25$^+$CD127$^-$ T cells) from PBMCs by FACS. Tconv is generally considered as the precursor cells of Treg. Therefore, the differentiation and amplification of Tconv were induced to iTreg by anti-CD3/CD28, IL-2, and TGF-β. The ratio of purified iTreg in CD4$^+$T cells was more than three times that of Tregs (Figure S2A). To further verify the suppressive effect on CD8$^+$T cells in vitro, we co-cultured iTregs and CD8$^+$T cells at the indicated ratio for 5 days. The results of FACS showed that the induced iTregs in vitro could suppress the proliferation of CD8$^+$T cells stained by CFSE (Figure S2B). Next, we verified whether lactate/GPR81 signaling could promote Treg migration in vitro. Supernatants from GC cells transfected with GPR81 shRNA or empty vector were collected for chemotaxis of iTregs in a transwell migration assay. Notably, the absolute count of
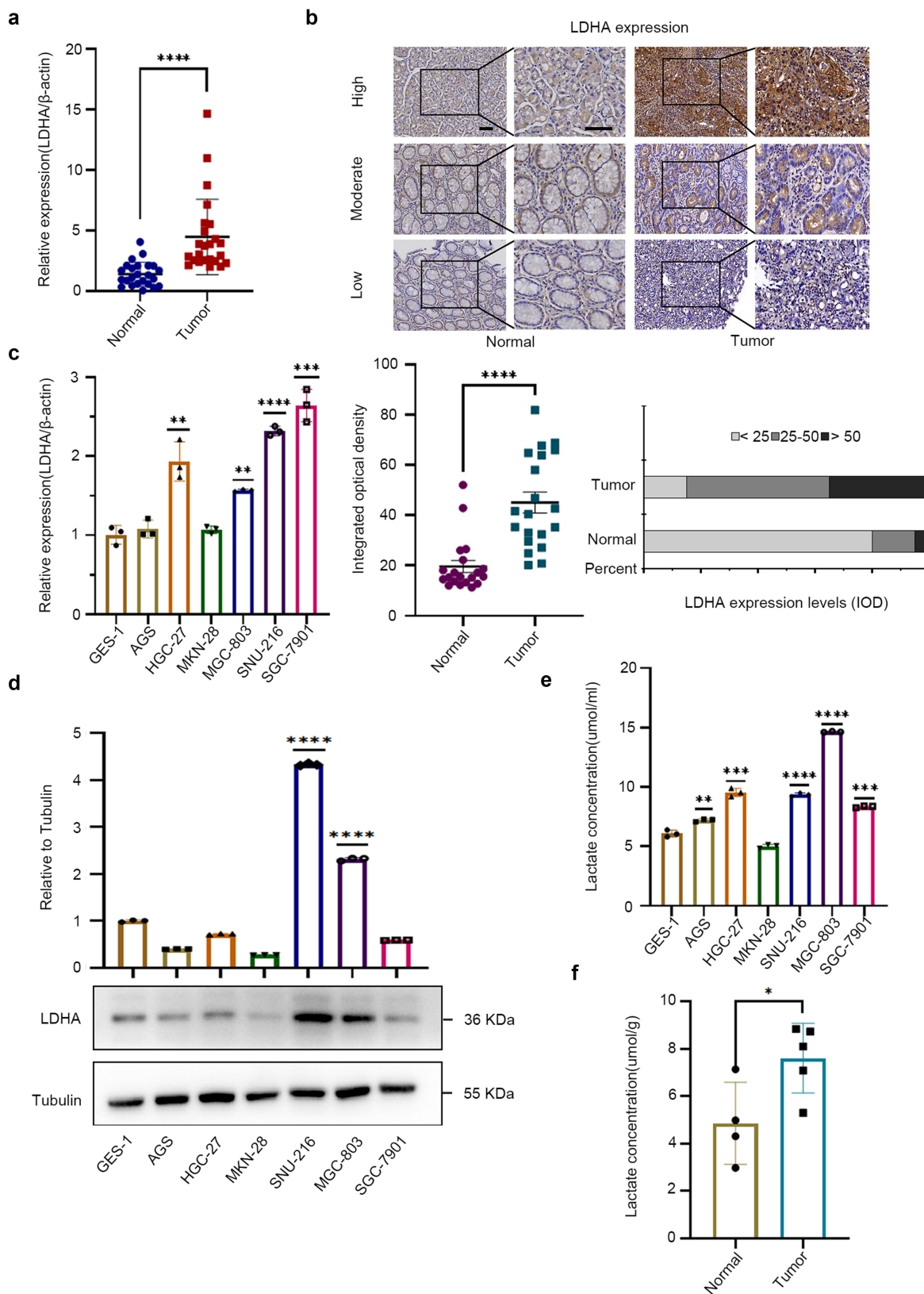
Figure 1. LDHA is upregulated in GC tissue and GC cells. (a) qPCR analysis of the LDHA mRNA in primary GC and adjacent normal tissues ($n = 24$, normalized to β-actin). (b) immunohistochemical images (above) and integrated optical density (IOD, below) comparison of LDHA in primary tumor and adjacent normal tissues of GC ($n = 20$). Scale bars, 100um. (c) qPCR analysis of LDHA mRNA of GC cells(AGS, HGC-27, MKN-28, SNU-216, MGC-803, and SGC-7901) and gastric epithelial cells(GES-1, normalized to β-actin, $n = 3$ biological replicates). (d) Western blot analysis of LDHA expression of GC cells (AGS, HGC-27, MKN-28, SNU-216, MGC-803, and SGC-7901) and GES-1 (normalized to tubulin, $n = 3$ biological replicates). (e) lactate concentration analysis of GC cells (AGS, HGC-27, MKN-28, SNU-216, MGC-803, and SGC-7901) and GES-1 supernatant after culture for 48 h. (f) lactate content detection of GC tissues ($n = 5$) and adjacent normal tissues ($n = 4$). Graphs show mean±SEM (a and b), and mean±SD (c and f). Statistical significance was calculated by two-tailed student's t-test (a, b, d, and f), one-way ANOVA with Tukey's post hoc (c and e). *$p < .05$; **$p < .01$; ***$p < .001$; ****$p < .0001$.
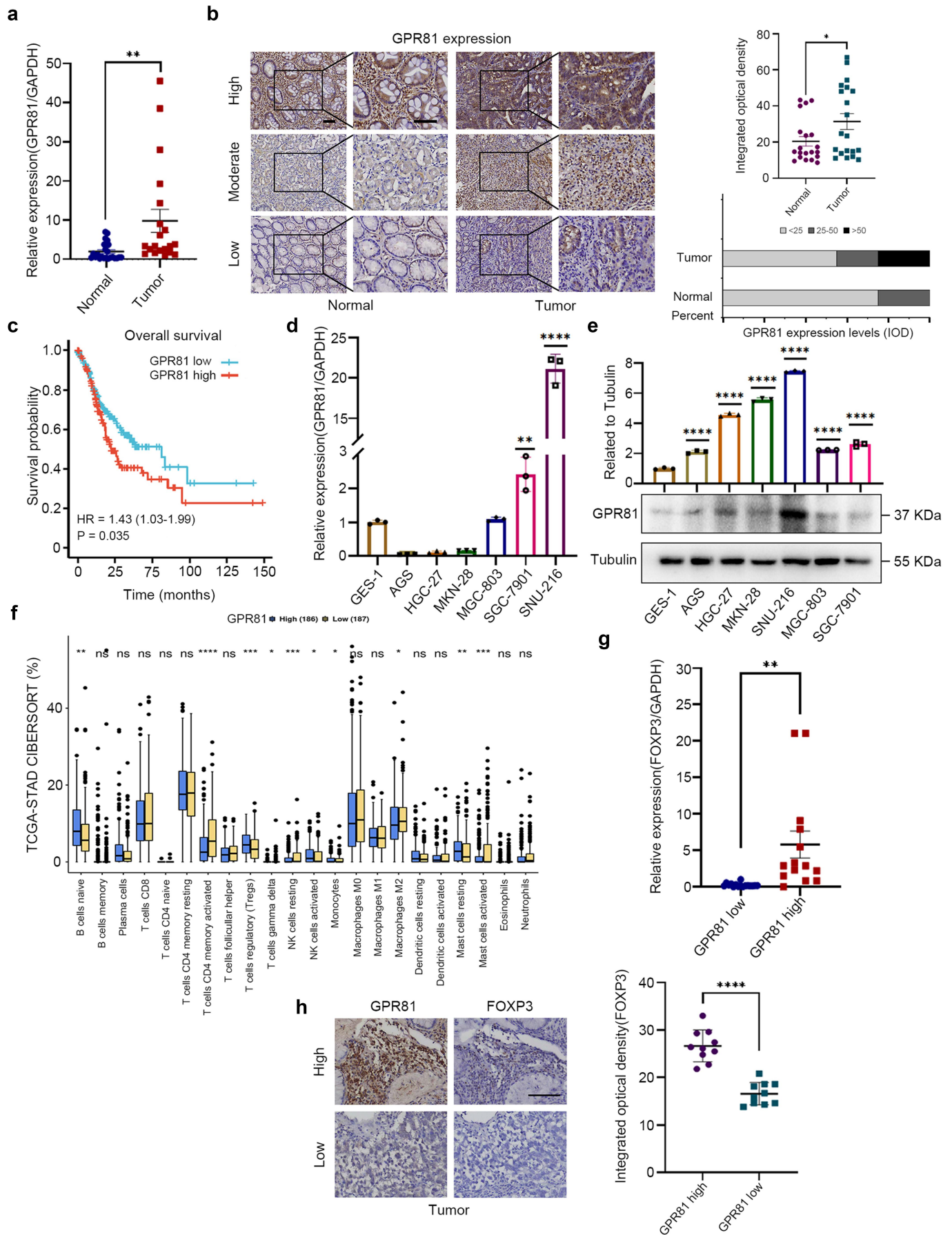
Figure 2. GPR81 is upregulated in GC tissues and GC cells, and correlated with poor prognosis and more Tregs infiltration of GC. (a) qPCR analysis of the GPR81 mRNA in primary GC tissues and adjacent normal tissues ($n = 24$, normalized to GAPDH). 4 outliers in the tumor group were excluded. (b) immunohistochemical images (left) and IOD (right) comparison of GPR81 in primary tumor and adjacent normal tissues of GC ($n = 20$). Scale bars, 100um. (c) overall survival curve of GPR81 high expression

iTregs migrating to the lower chamber decreased after SGC-7901 was transfected with GPR81 shRNA (Figure 4(a)). Moreover, migration assay in PBMCs was performed, and the results of FACS illustrated that the ratio of Tregs in total CD4+T cells was significantly decreased when GPR81 was knocked down. Similarly, the ratio of Tregs to CD8+T cells declined when transfected with GPR81 shRNA. However, we found no significant difference in the ratio of CD8+T cells in PBMCs between the groups (Figure 4(b)). To further confirm the results, plasmids overexpressing GPR81 were transfected in GC cells (Figure 4(c)). In contrast, the ratio of Tregs in total CD4+T cells and Tregs to CD8+T cells were both significantly increased (Figure 4(d)), suggesting a specific modulation of lactate/GPR81 signaling on Tregs recruitment.

To confirm whether the recruitment effect of Tregs was caused by lactate/GPR81 signaling through modulating CX3CL1, we initially explored the chemotaxis of CX3CL1 to iTregs through in vitro transwell migration assay. Interestingly, the absolute count of migrated iTreg to the lower chamber increased with the rise in the concentration of CX3CL1 gradually (Figure 4(e)). Furthermore, migration assay implied that the ratio of Tregs in total CD4+T cells and Tregs to CD8+T cells significantly increased under the condition of incubation with a specific concentration of CX3CL1, while the ratio of CD8+T cells in PBMCs in the lower chamber showed no significant difference between the two groups (Figure 4(f)). It suggested that CX3CL1 exhibited chemotaxis on Tregs but not on CD8+T cells in vitro. In addition, siRNA was transfected into GC cell lines to knock down CX3CL1. Western blot analysis showed that CX3CL1 protein levels were significantly decreased after being transfected with CX3CL1 siRNA (Figure 4(g)). FACS analysis indicated that the ratio of Tregs in total CD4+T cells and Tregs to CD8+T cells significantly decreased after incubation with supernatants collected from GC cells transfected with CX3CL1 siRNA (Figure 4(h)). Taken together, lactate/GPR81 might modulate CX3CL1 expression and trigger Tregs recruitment without affecting CD8+T cell migration.

Lactate/GPR81 regulated CX3CL1 expression to promote Tregs migration by activating p65

We next investigated the specific molecular mechanism of lactate/GPR81 modulating CX3CL1 expression. The GPR81 knockdown and overexpression models of GC cell lines were established by transfection with corresponding plasmids. Western blot analysis suggested that the phosphorylated p65 and downstream CX3CL1 expressions were both decreased when GPR81 was knocked down and increased when it was overexpressed (Figure 5a). Consistently, phosphorylated p65 and the downstream CX3CL1 expressions were increased after incubation with lactate at the indicated concentration in SGC-7901 and SNU-216 (Figure 5(b)). These results were also verified in human GC samples. IHC analysis of sequential pathological sections of GC tissues found that the region with increased GPR81 expression also had high expressions of phosphorylated p65, CX3CL1, and FOXP3 (Figure 5(c)), confirming the positive regulation of lactate/GPR81 to p65 and CX3C1L.

We further explored whether p65 had a positive correlation with CX3CL1 expression and Tregs migration. To this end, RT-qPCR and Western blot were performed after SGC-7901 cells were transfected with p65 siRNA or empty control. The expression of CX3CL1 decreased after p65 was knocked down than that in the control group (Figure 5(d)). Consistently, Elisa analysis implied that the concentration of CX3CL1 from the supernatants of SGC-7901 and SNU-216 decreased after interfered with p65 siRNA (Figure 5(e)). Moreover, transwell migration assay confirmed that the ratio of Tregs in total CD4+T cells and Tregs to CD8+T cells were both significantly decreased after co-cultured with the supernatants of SGC-7901 transfected with p65 siRNA (Figure 5(f)). With GPR81 knocked down, the phosphorylated p65 and downstream CX3CL1 remained at low levels in GC cells after being stimulated by lactate and showed no significant increase when the concentration of lactate gradually raised (Figure S3A). In contrast, the protein expression of CX3CL1 was upregulated when SGC-7901 and SNU-216 were stimulated with p65 activator lipopolysaccharide (LPS) (Figure 5(g)). Interestingly, the down-regulated CX3CL1 was reversed by LPS in GC cell lines after being transfected with GPR81 shRNA (Figure 5(h)). Meanwhile, the knockdown of p65 could reverse the up-regulated CX3CL1 after overexpressing GPR81 or lactate incubation in SGC-7901 (Figure 5(i), S3B). In summary, the activation of lactate/GPR81 signaling might phosphorylate p65 and modulate the expression of CX3CL1, and the secreted CX3CL1 to the TME can trigger the directional migration of Tregs.

Phosphorylated p65 translocates bound to the promoter of CX3CL1 in GC cells

To examine whether p65 bound to the transcription start site of CX3CL1, we extracted the cytoplasmic protein and nuclear protein respectively. Interestingly, the results of the Western blot showed that the detected p65 protein levels were higher in the nucleus than in the cytoplasm as the GPR81 was overexpressed in GC cells. However, when SNU-216 and MGC-803 were transfected with plasmids that expressed GPR81 shRNA, a higher level of p65 was found in the cytoplasm than in the nucleus (Figure 6(a)).

group and GPR81 low expression group of GC patients from TCGA ($n = 443$). (d) qPCR analysis of GPR81 mRNA of GC cells (AGS, HGC-27, MKN-28, SNU-216, MGC-803, and SGC-7901) and GES-1 (normalized to GAPDH, $n = 3$ biological replicates). (e) Western blot analysis of GPR81 expression of GC cells (AGS, HGC-27, MKN-28, SNU-216, MGC-803, and SGC-7901) and GES-1 (normalized to tubulin, $n = 3$ biological replicates). (f) correlation between GPR81 expression and tumor-infiltrating lymphocytes of GC tissues (GPR81 high group, $n = 186$, GPR81 low group, $n = 187$). (g) qPCR analysis of the FOXP3 mRNA of the GPR81 high expression group ($n = 15$) and GPR81 low expression group ($n = 16$) of GC patients (normalized to GAPDH). 1 outlier in the GPR81 high-expression group was excluded. (h) immunohistochemical images (left) and IOD (right) comparison of FOXP3 between GPR81 high expression group and GPR81 low expression group in primary tumor tissues of GC ($n = 20$). Scale bars, 100um. Graphs show mean±SEM (a and b), and mean±SD (d and h). Statistical significance was calculated by two-tailed student's t-test (a, b, e, g, and h), one-way ANOVA with Tukey's post hoc (d), log-rank analysis (c), and Wilcoxon test (f). *$p < .05$, **$p < .01$; ***$p < .001$; ****$p < .0001$.
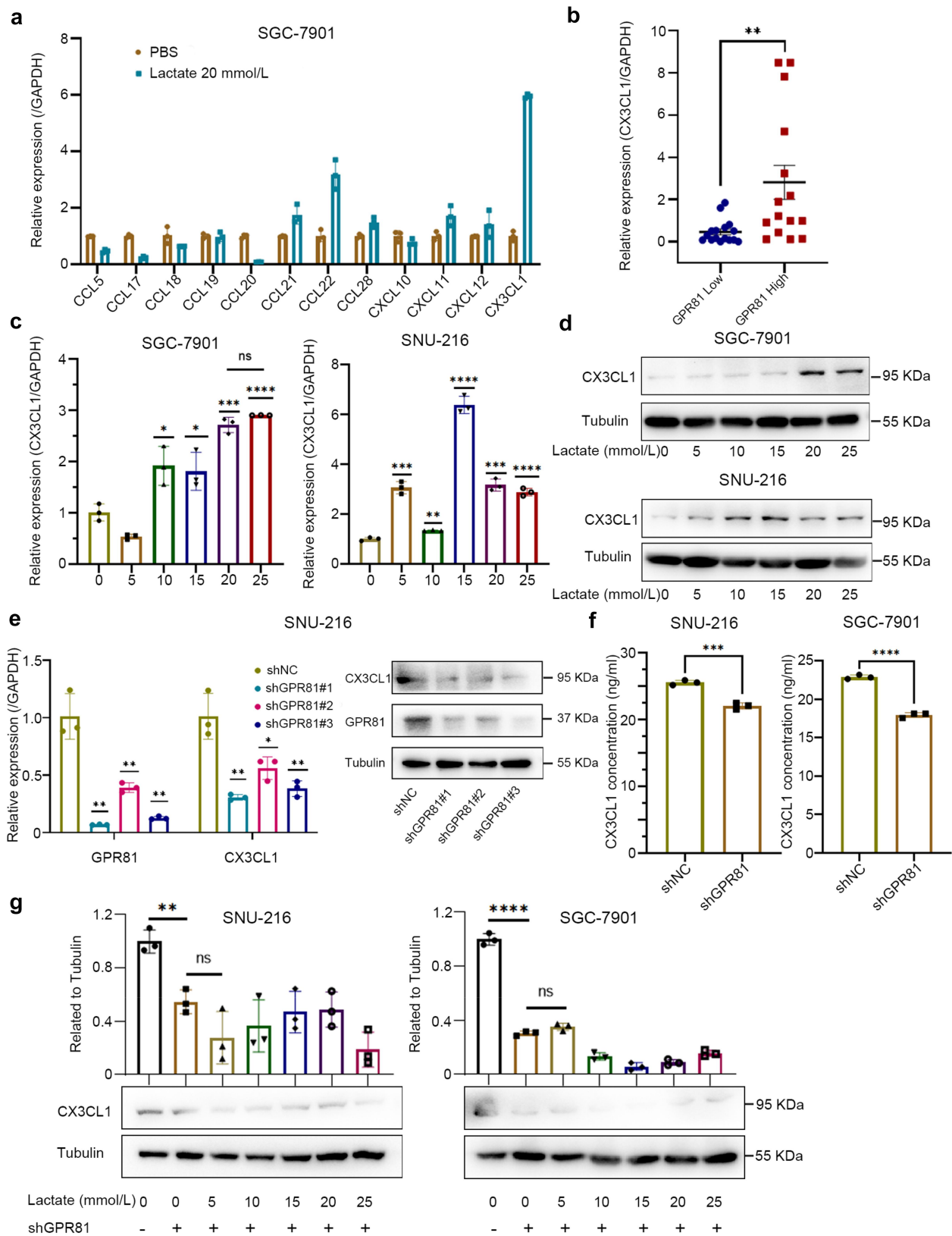
Figure 3. Lactate/GPR81 modulates chemokine CX3CL1 expression in a concentration-dependent manner in GC cells. (a) qPCR analysis of the expression of the chemokines in SGC-7901 incubated with lactate (20 mmol/L) for 6 h (normalized to GAPDH, $n = 3$ biological replicates). (b) qPCR analysis of the CX3CL1 mRNA of the GPR81 high expression group ($n = 15$) and GPR81 low expression group ($n = 16$) of GC patients (normalized to GAPDH). (c) qPCR analysis of the CX3CL1 mRNA of GC cells (SGC-7901, SNU-216) incubated with the indicated concentration of lactate for 6 h (normalized to GAPDH, $n = 3$ biological replicates). (d) Western blot analysis of the CX3CL1 expression of GC cells (SGC-7901, SNU-216) incubated with the indicated concentration of lactate for 6 h. (e) qPCR (left) and Western blot (right) analysis of the relationship between GPR81 and CX3CL1 in GC cells after transfected with plasmids expressing shRNA against GPR81. (f) CX3CL1 concentration was detected by Elisa of GC cells (SGC-7901, SNU-216) culture supernatant after transfected with plasmids expressing shRNA against GPR81. (g) Western blot analysis for CX3CL1 in GC cells (SGC-7901, SNU-216) incubated with the indicated concentration of lactate for 6 h after transfected with shRNA against GPR81. Graphs show mean±SEM (b), and mean±SD (a, c, e and g). Statistical significance was calculated by two-tailed student's t-test (b and f), one-way ANOVA with Tukey's post hoc (c, e, and g). $*p < .05$, $**p < .01$; $***p < .001$; $****p < .0001$.
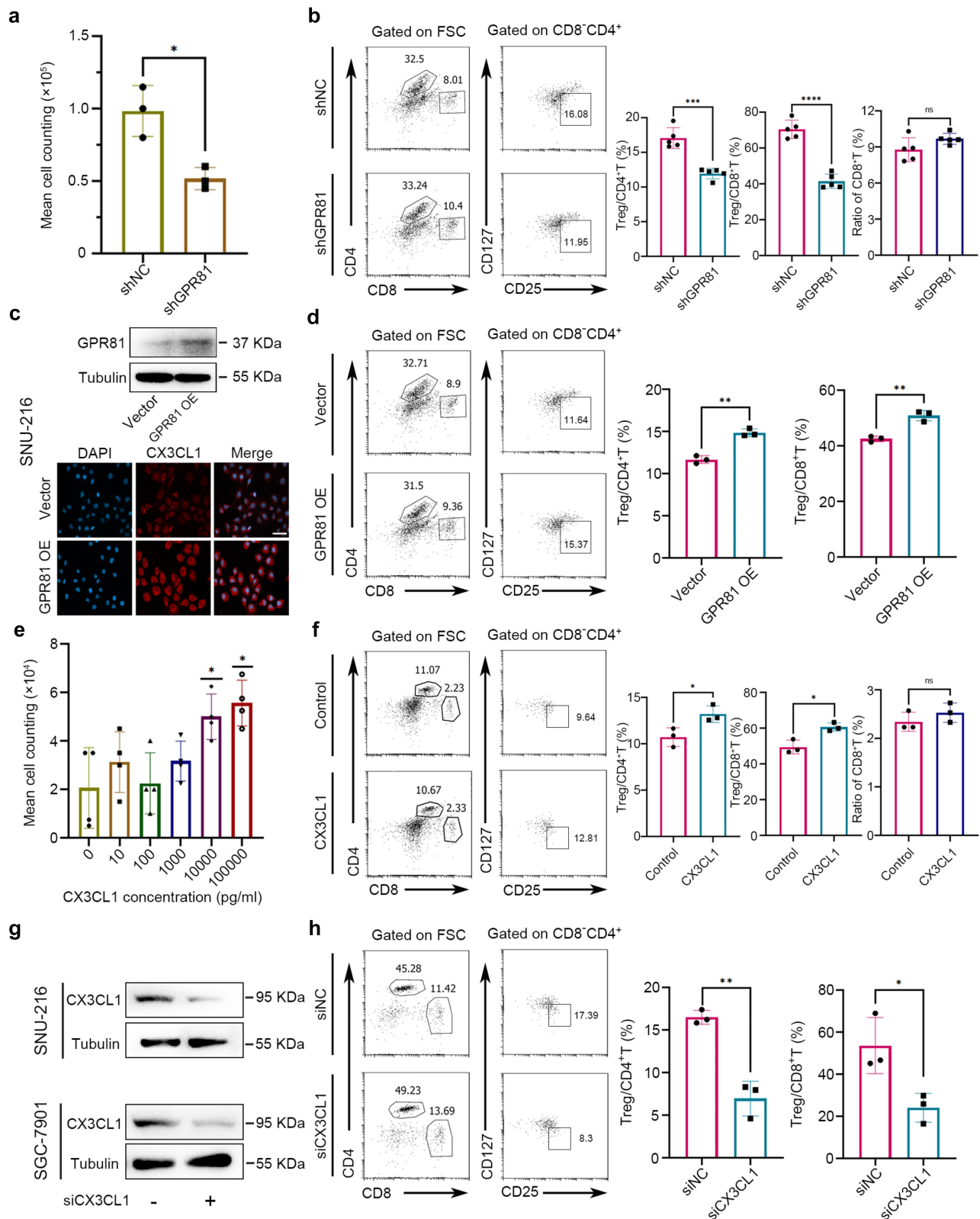
Figure 4. Lactate/GPR81 chemotaxis Tregs by modulating the expression of chemokine CX3CL1. (a) the absolute number of migrated iTregs to the lower chamber after co-culturing with SGC-7901 supernatant transfected with shRNA against GPR81 for 6 h. (B) flow cytometry analysis of $CD8^-CD4^+CD25^+CD127^-$ cells (Tregs) and $CD8^+T$ cells ratio in PBMCs which migrate to the lower chamber after co-cultured with GC cell supernatant transfected with GPR81 shRNA for 6 h. (c) Representative images of Western blot (above) and immunofluorescence (below) in SNU-216 after transfected with GPR81 overexpression plasmids and vector plasmids. Cells were stained with CX3CL1 (red) and nuclei with DAPI (blue). Scale bars, 50 μm. (d) flow cytometry analysis of Tregs and $CD8^+T$ cells ratio in PBMCs which were migrated to the lower chamber after co-cultured with GC cell supernatant transfected with GPR81 plasmids for 6 h. (e) iTregs migration with the indicated concentration of CX3CL1 in vitro. (f) flow cytometry analysis of Tregs and $CD8^+T$ cells ratio in PBMCs which were migrated to the lower chamber after co-culturing with a specific concentration of CX3CL1 for 6 h. (g) Western blot analysis of CX3CL1 expression in GC cells (SGC-7901, SNU-216) after transfected with siRNA against CX3CL1. (h) flow cytometry analysis of Tregs and $CD8^+T$ cells ratio in PBMCs which migrate to the lower chamber after co-cultured with GC cell supernatant transfected with siRNA against CX3CL1 for 6 h. Graphs show mean±SD (a-f, and h). Statistical significance was calculated by two-tailed student's t-test (a, b, d, f, and h), one-way ANOVA with Tukey's post hoc (e). *p < .05, **p < .01; ***p < .001; ****p < .0001.
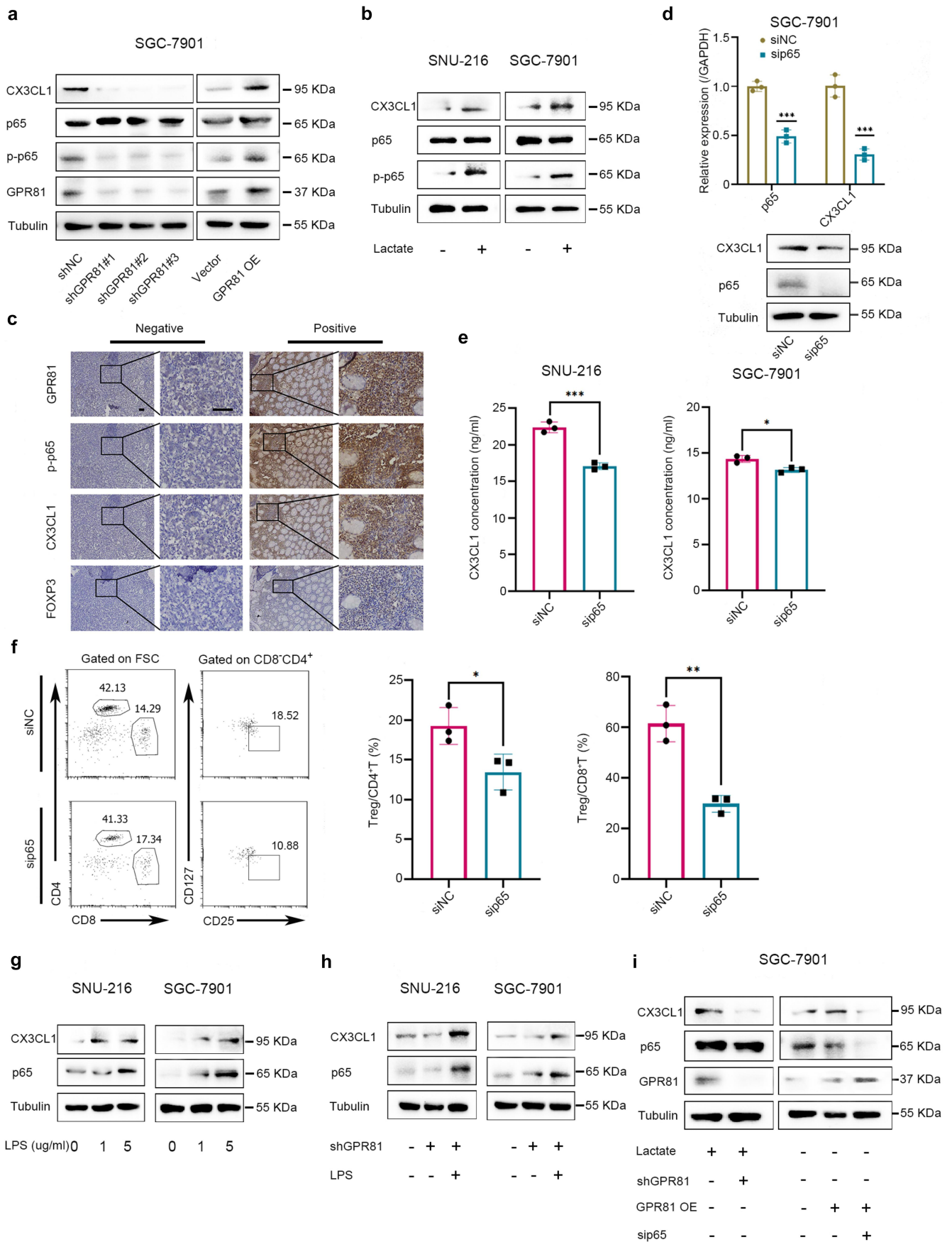
Figure 5. Lactate/GPR81 regulates CX3CL1 to promote Tregs migration by activating p65. (a) Western blot analysis of GPR81, p65, p-p65, and CX3CL1 in SGC-7901 after transfected with plasmids expressing shRNA against GPR81 (normalized to tubulin, $n = 3$ biological replicates). (b) Western blot analysis of GPR81, p65, p-p65, and CX3CL1 in GC cells (SGC-7901, SNU-216) incubated with lactate for 6 h (normalized to tubulin, $n = 3$ biological replicates). (c) Representative immunohistochemical images of correlation between GPR81, p-p65, CX3CL1, and FOXP3 in GC tissues. Scale bars, 100 μm. (d) qPCR (above) and Western blot (below) analysis of the relationship between

Verification of the translocation of p65 by immunofluorescence is shown in Figure 6(b). Next, a dual luciferase reporter assay was performed in SGC-7901 and MGC-803, which transfected with or without GPR81 overexpressing plasmids. The results indicated that GPR81 elevated the activity of the CX3CL1 promoter (Figure 6(c)). Moreover, the reporter activity of CX3CL1 was decreased in SGC-7901 and MGC-803 when p65 was knocked down by siRNA (Figure 6(c)). Collectively, p65 might be the transcriptional factor of CX3CL1 and promote its expression in GC cells.

The infiltrated Tregs combined with lactate in TME promoted the immunosuppression by inhibiting the killing effect of CD8+T cells

CD8+T cells play a pivotal role in tumor immunology and have direct killing effects on tumor cells. The ratio of Tregs and CD8+T cells in TME can indicate the efficiency of anti-tumor immunity. CD8+T cells were sorted from PBMCs and co-cultured with SGC-7901 and SNU-216 in indicated proportion. The killing effects on GC cells enhanced as the ratio of CD8+T cells to GC cells increased (Figure 7(a)). Next, we co-cultured SGC-7901 cells with a specific proportion of iTregs and CD8+T cells for 48 h. The cytotoxicity of CD8+T cells to SGC-7901 was analyzed by CCK8 assay. As shown in Figure 7(b), the killing effects of CD8+T cells to GC cells decreased as the ratio of iTregs to CD8+T cells increased. The results of the plate cloning assay were consistent with those of the CCK8 assay, indicating that Tregs could inhibit the function of CD8+T cells to suppress GC cell growth in a quantity-dependent manner (Figure 7(c)). For further verification, RT-qPCR was performed after the co-culture of iTreg with SGC-7901 supernatant for 24 h. Tumor-related iTregs were detected with higher expressions of FOXP3, TGF-β, and IL-10 than those of the control (Figure 7(d)), suggesting that tumor-infiltrated iTregs posed a stronger immunosuppressive effect.

Furthermore, we co-cultured CD8+T cells with SNU-216 and MGC-803 with or without the indicated concentration (20 mmol/L) of lactate for 48 h. CCK8 assay was performed to detect the surviving cells after PBS was washed twice. According to the results of the CCK8 assay, exogenous lactate weakened the killing effects of CD8+T cells on GC cells (Figure 7(e)). Compared with the group without lactate added, there was a significant increase in the colonies plated from the remnant SGC-7901 after co-culture with CD8+T cells and incubation with lactate at the indicated concentration (Figure 7(f)). Together, the GC-infiltrated Tregs and lactate from the GC cells might co-construct the immunosuppressive TME.

GPR81 blockage inhibited Tregs tumor-infiltration to suppress GC progression in vivo

We further elucidated whether GPR81 blockage could indeed inhibit GC progression by decreasing Tregs infiltration in vivo. A humanized mouse model was established by PBMC administration through the tail vein.[31] Blood was sampled from the posterior orbital venous plexus of NOD.Cg-Prkdc^scid IL2rg^em1Smoc (M-NSG) mice before and after PBMCs injection. FACS analysis showed a robust level of CD45+CD3+ cells in the peripheral blood of mice after 21 days of engraftment (Figure S4).

Next, we established a subcutaneous heterograft tumor model in M-NSG mice, and reconstituted the immune system 5 to 7 days after GC cell injection (Figure 8(a)). MGC-803 with GPR81 was knocked down by lentivirus, and the result was verified by Western blot (Figure 8(b)). The subcutaneous tumor was captured and analyzed on day 29. Mice transplanted with GC cells after GPR81 knockdown showed reduced tumor volumes compared with those of the control group. Simultaneously, the proliferation of tumor cells decreased in the GPR81 knockdown group, and the difference began on day 16 after PBMC administration (Figure 8(c)). IHC of continuous sections indicated that the co-expression of phosphorylated p65, CX3CL1, and FOXP3 was observed in the same location of the two groups (Figure 8(d)). Single-cell suspension was prepared after the subcutaneous tumor was captured. The results showed that the ratio of Tregs in total CD4+T cells decreased among tumor-infiltrated lymphocytes after the knockdown of GPR81 (Figure 8(e)). Meanwhile, the intratumoral Tregs to CD8+T cells declined at the same time, suggesting that lactate/GPR81 signaling blockage might inhibit Tregs intratumoral recruitment and revealed little chemotaxis to CD8+T cells. In short, these data illustrated that Tregs might migrate into intratumoral region and contribute to GC progression depending on lactate/GPR81 signaling activity.

Discussion

The acidic micro-environment caused by lactate accumulation in extracellular surroundings plays a crucial role in the anti-tumor immune response. Tregs are a highly suppressive subgroup of CD4+T cells and the dominant composition of the immunosuppressive microenvironment.[21,32] Prior evidence suggested that Tregs frequencies in TME possessed prognostic properties in GC.[33] Therefore, understanding the molecular mechanism of lactate and Tregs infiltration is urgently needed to design therapies for target lactate signaling and Tregs. In the present study, tumor-derived lactate bound to its receptor GPR81 to promote Tregs infiltration by modulating

---

p65 and CX3CL1 in SGC-7901 after transfected with siRNA against p65 (qPCR normalized to GAPDH, Western blot normalized to tubulin, $n = 3$ biological replicates). (e) CX3CL1 concentration was detected by Elisa in GC cells (SGC-7901, SNU-216) culture supernatant after transfected with siRNA against p65. (f) flow cytometry analysis of CD8−CD4+CD25+CD127− cells (Tregs) and CD8+T cells ratio in PBMCs which migrate to the lower chamber after co-cultured with GC cell supernatant transfected with siRNA against p65 for 6 h. (g) Representative Western blot images of correlation between p65 and CX3CL1 in GC cells (SGC-7901, SNU-216) after stimulated by LPS for 4 h (normalized to tubulin, $n = 3$ biological replicates). (h) Western blot analysis of p65 and CX3CL1 in GC cells (SGC-7901, SNU-216) stimulated by LPS for 4 h after transfected with plasmids expressing shRNA against GPR81 (normalized to tubulin, $n = 3$ biological replicates). (i) Western blot analysis of p65 and CX3CL1 in SGC-7901 incubated with lactate for 6 h after transfected with plasmids expressing shRNA against GPR81 or transfected with plasmids overexpressing GPR81 or transfected with siRNA against p65 (both normalized to tubulin, $n = 3$ biological replicates). Graphs show mean±SD (d-f). Statistical significance was calculated by two-tailed student's t-test (d and f). $*p < .05$, $**p < .01$; $***p < .001$.
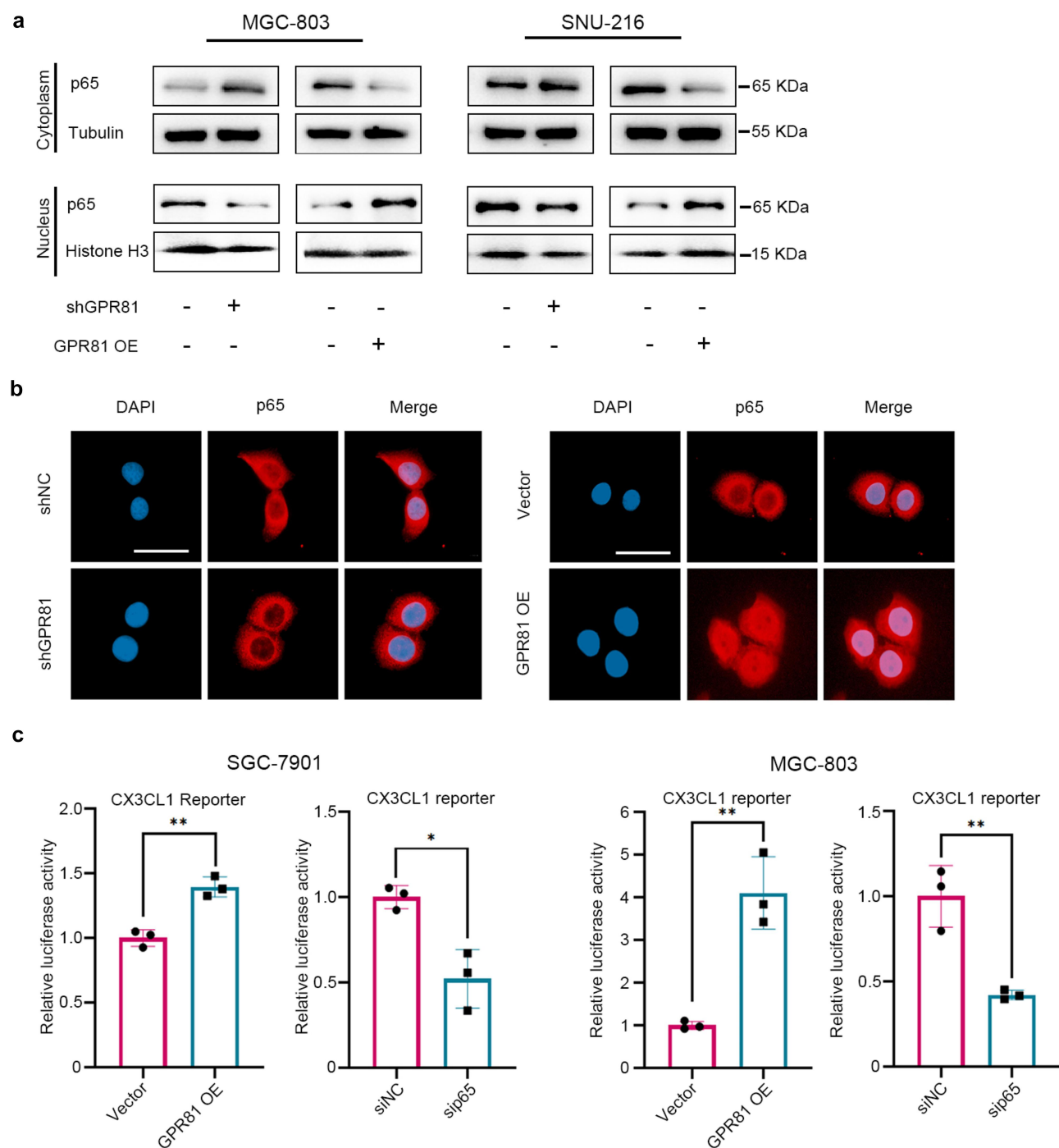
a

b

c

Figure 6. Phosphorylated p65 translocates to the nucleus and binds to the promoter of CX3CL1 in GC cells. (a) Western blot analysis for p65 distribution in the cytoplasm and nucleus of GC cells (MGC-803, SNU-216) after transfected with plasmids expressing shRNA against GPR81 or transfected with GPR81 overexpressed plasmids (cytoplasm normalized to tubulin, nucleus normalized to histone H3, $n = 3$ biological replicates). (b) Representative immunofluorescence images for p65 distribution in the cytoplasm and nucleus of SNU-216 after transfected with plasmids expressing shRNA against GPR81 or transfected with GPR81 overexpressed plasmids. Scale bars, 50 μm. (c) Dual-luciferase reporter activities for CX3CL1 promoter in GC cells (SGC-7901, MGC-803) after transfected with plasmids that overexpression of GPR81 or with siRNA that against p65 expression ($n = 3$ biological replicates). Graphs show mean±SD (c). Statistical significance was calculated by a two-tailed student's t-test (c). *$p < .05$, **$p < .01$.

chemokine CX3CL1 expression. Accordingly, targeting the lactate/GPR81 signaling to reverse the status of immunosuppression in TME may serve as a potential therapeutic strategy for GC.

Lactate is the metabolic product of glycolysis, and transports to extracellular stroma by monocarboxylate transporters (MCTs).[5,34] The concentration of lactate can be remarkably elevated up to 40 mmol/g in glycolytic tumors.[35] High concentrations of lactate in TME are associated with tumor progression, distant metastases, and poor outcomes.[36–39] We found that GC is a highly glycolytic tumor with overexpressed LDHA and high concentration of lactate. High levels of lactate in TME attenuate the killing effects of CD8^{+}T cells on GC cells. The tumor-promoting function of lactate/MCT1 signaling has been
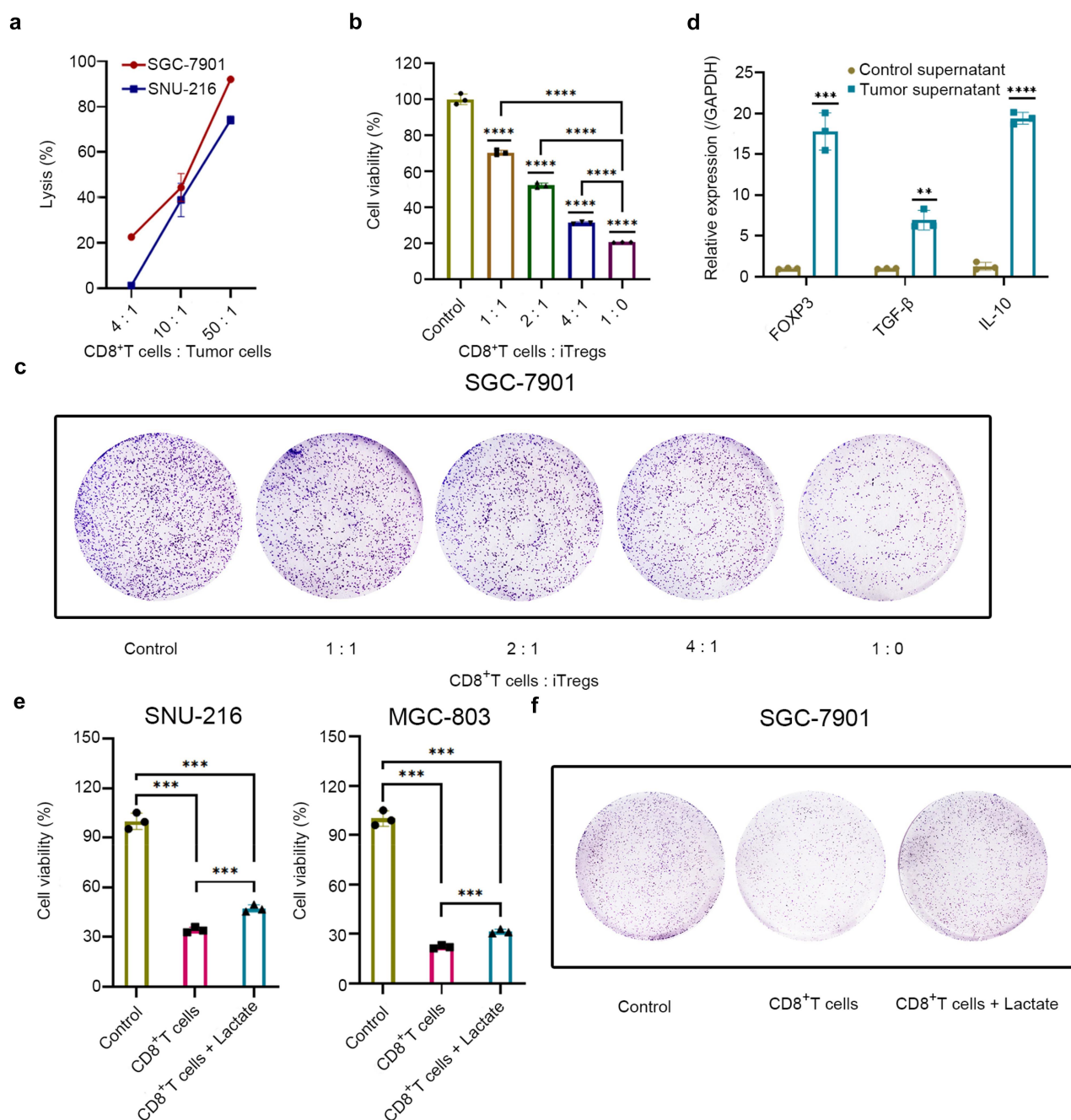
Figure 7. The infiltrated Tregs enhance immunosuppression by inhibiting the killing effect of CD8^{+}T cells. (a) cytotoxicity of CD8^{+} T cells against GC cells (SGC-7901, SNU-216) co-culture for 48 h at the indicated ratio. (b) cytotoxicity of CD8^{+} T cells against SGC-7901 when co-culture with iTregs at the indicated ratio. (c) Representative well images for SGC-7901 colonies plated from remnant SGC-7901 after co-culture with CD8^{+}T cells and iTregs at the indicated ratio for 48 h. (d) qPCR analysis for FOXP3, TGF-β, and IL-10 in iTregs after co-culture with GC cells supernatant versus control supernatant for 24 h (normalized to GAPDH, $n = 3$ biological replicates). (e) cytotoxicity of CD8^{+} T cells against GC cells (SGC-7901, MGC-803) after co-culture with CD8^{+}T cells at the specific ratio (CD8^{+}T cells : GC cells is 20 : 1) with or without lactate (20 mmol/L) incubation for 48 h. GC cells that had not been treated as the control. (f) Representative well images for SGC-7901 colonies plated from remnant SGC-7901 after co-culture with CD8^{+}T cells at the indicated ratio with or without lactate (20 mmol/L) incubation for 48 h. Graphs show mean±SD (a, b, d, and e). Statistical significance was calculated by two-tailed student's t-test (d), one-way ANOVA with Tukey's post hoc (b and e). **$p < .01$; ***$p < .001$; ****$p < .0001$.

broadly reported.[40,41] However, lactate combined with GPR81 could modulate the presentation of MHC II on the surface of dendritic cells and reinforce the immunosuppression of myeloid-derived suppressor cells (MDSCs).[42,43] As an autocrine, lactate can bind to GPR81 to upregulate PD-L1, thereby blocking T cell recognition in human lung cancer.[44] In this text, GPR81 is highly expressed in GC and correlated with poor prognosis in GC patients. To further clarify whether lactate/GPR81 signal drives immune resistance in GC, we explored the data from the TCGA and found that the expression of GPR81 was positively correlated with tumor infiltration of Tregs. Similarly, we observed that the GPR81 high expression group with higher FOXP3 expression in GC samples. GPR81 blockage in GC cells reduced the migration of Tregs. In contrast, Tregs migration increased when GPR81 was overexpressed. Surprisingly, the status of GPR81 made no difference to
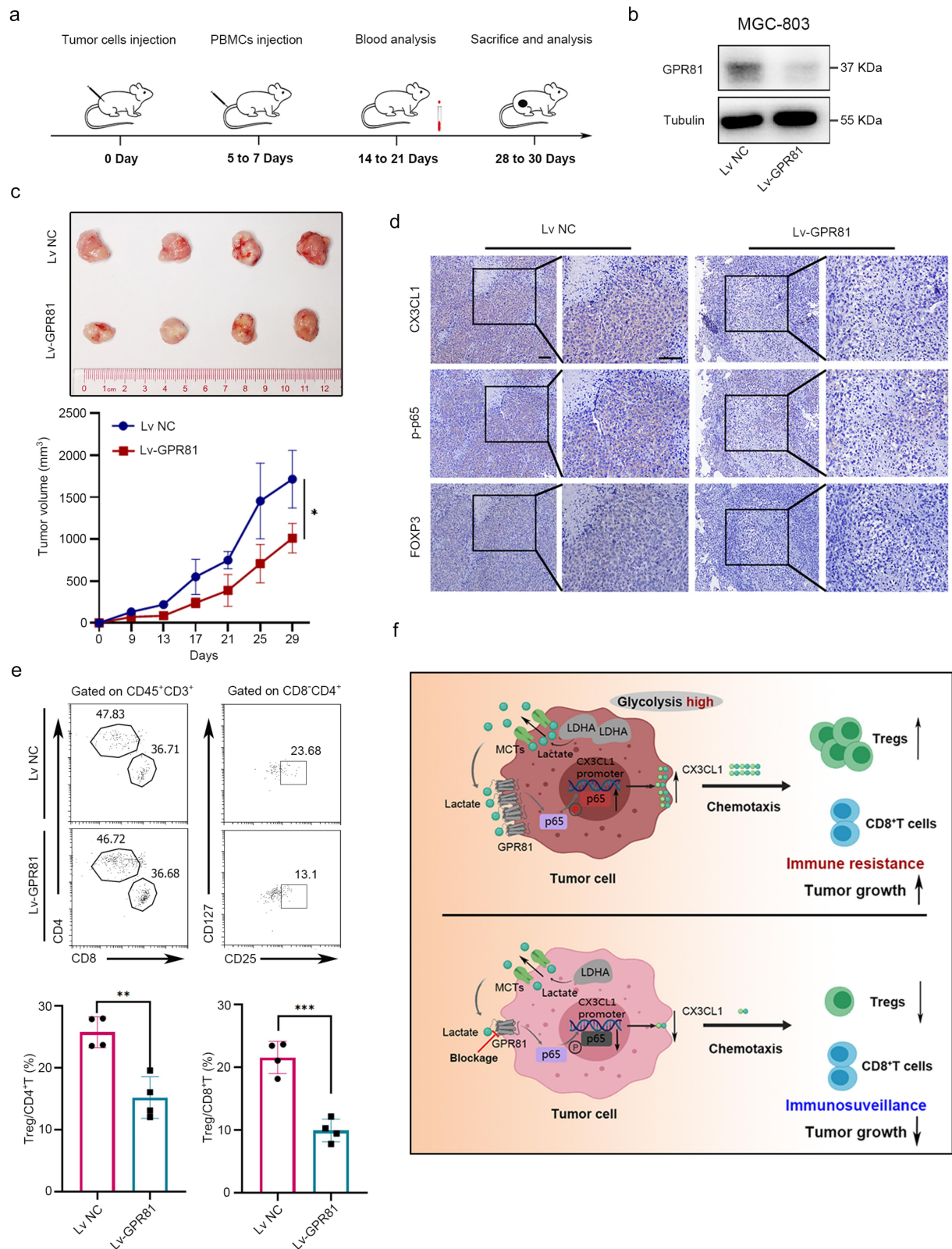
Figure 8. GPR81 blockage inhibits Tregs recruitment and GC progression. (a) scheme induction of GC subcutaneous tumor model in the humanized NOD.Cg-Prkdc[scid] IL2rg[em1Smoc] (M-NSG) mice. The time of tumor cell injection was recorded as day 0. The healthy donors' PBMC was injected through the tail vein on days 5 to 7 to construct a humanized mice model. Venae orbitalis posterior blood was sampled in mice to evaluate humanized efficiency on days 14 to 21. The subcutaneous tumor was captured for analysis on days 28 to 30. (b) Western blot analysis of GPR81 in MGC-803 after transfected with lentivirus (lv) against GPR81 or empty lentivirus (normalized to tubulin, $n = 3$ biological replicates). (c) the described data is represented as tumor volumes (above), and tumor volume curve (below) in mice (4 mice per group) after being injected with MGC-803 transfected with lentivirus against GPR81 or empty lentivirus. (d) immunohistochemical analysis of the correlation between CX3CL1, p-p65, and FOXP3 in MGC-803 subcutaneous tumor. Scale bars, 200 μm. (e) flow cytometry analysis of the CD45^{+}CD3^{+}CD8^{−}CD4^{+}CD25^{+}CD127^{−} cells (Tregs) and CD8^{+}T cells ratio in tumor-infiltrating lymphocytes separated from single cell suspension of the subcutaneous tumor. (f) Lactate/GPR81 recruits Tregs by regulating CX3CL1 expression, thereby creating an immunosuppressive tumor microenvironment to promote tumor progression by inhibiting the activity of CD8^{+}T cells. Graphs show mean±SD (c and e). Statistical significance was calculated by two-tailed student's t-test (e), 2-way ANOVA followed by correction for multiple comparisons (c). *p < .05, **p < .01; ***p < .001.

CD8$^+$T cells migration and GC cells proliferation. In addition, GPR81 elimination inhibited GC growth by decreasing tumor infiltration of Tregs in a humanized mouse model. These data imply that the immune tolerance caused by lactate/GPR81 signaling in GC was aroused by Tregs infiltration. One possible explanation for Tregs infiltration is that lactate/GPR81 regulates the expression of specific chemokines, which needs further investigations.

Chemokines in TME are indispensable for Tregs recruitment.[45,46] In lung adenocarcinoma, epidermal growth factor receptor (EGFR) mutation was positively correlated with abundant Tregs infiltration by up-regulating CCL20 expression.[47] The abnormal activation of β-catenin upregulated CCL28 and subsequently increased the recruitment of tumor Tregs to accelerate GC development.[26] In addition, the expression of focal adhesion kinase (FAK) in squamous cell carcinoma could induce tumor progression through the increased infiltration of Tregs, which was recruited by CCL5.[48] However, it is still unclear concerning the main chemokines in an acidic TME. We found that multiple chemokines elevated after incubation with lactate for 6 h in several GC cell lines, among which CX3CL1 increased the most remarkably. The expression of CX3CL1 in GC cells was concentration-dependent with lactate. The same results were also observed in human breast cancer cells and colon cancer cells. We further found that the expression of GPR81 was positively correlated with the expression of CX3CL1. The up-regulated CX3CL1 by lactate was interrupted after GPR81 knockdown. These data indicate that CX3CL1 is the main chemokine in a highly glycolytic TME and is regulated by lactate/GPR81 signaling. CX3CL1 was previously reported to be correlated with intraepithelial lymphocyte recruitment of the intrahepatic bile duct.[49] In recent years, CX3CL1 was found positively correlated with tumor infiltration of macrophages, MDSCs, and NK cells to promote tumor progression in various malignant tumors.[50–52] Whether CX3CL1 had chemotaxis on Tregs tumor infiltration was rarely reported. According to the present study, the expression of CX3CL1 was related to FOXP3 expression in GC samples. Exogenous CX3CL1 promoted Tregs migration in a transwell assay. While depleting CX3CL1 in GC cells hindered the migration of Tregs. Moreover, the ratio of CD8$^+$T cells migrated to the low chamber exhibited no significant change after CX3CL1 depletion. These results imply that lactate/GPR81 can promote Tregs infiltration by regulating CX3CL1 expression. Further investigations are needed to fully clarify the mechanisms for transcriptional regulation of CX3CL1 expression in GC.

Elevated activity of NF-κB signaling has been documented to be correlated with the tumorigenesis of inflammation-based cancersand is involved in tumor proliferation, metastasis, and resistance to apoptosis.[53,54] p65 is the subunit of the NF-κB family. In human bladder cancer, p65 was reported to be related to tumor invasion due to the modulatory effect on matrix metalloproteinase-13 expression.[55] The inhibition of NF-κB may promote cancer cell apoptosis and significantly delay tumor growth.[56] Moreover, NF-κB signaling can regulate the expression of chemokine CCL20, which recruits Tregs to promote immune tolerance in TME.[22] We found that p65 was essential for CX3CL1 expression regulated by lactate/GPR81 signaling. The status of phosphorylated p65 was consistence with the expression of CX3CL1 and GPR81 in GC samples. These results were also confirmed in a humanized mouse model. The activated p65 translocated to the nucleus and bound to the promoter sequence of CX3CL1, hence regulating the transcription and translation of CX3CL1. Furthermore, Tregs migration decreased after p65 depletion in GC cells. On the contrary, Tregs migration increased when p65 was activated. As suggested by our research, lactate/GPR81/p65/CX3CL1 axis is required for Tregs infiltration in GC.

In summary, this study presents a fresh insight that lactate/GPR81 recruits Tregs to reshape an immunosuppressive TME in highly glycolytic GC (Figure 8(f)). The blockage of lactate/GPR81/p65/CX3CL1 signaling may serve as a potentially novel therapeutic strategy for the treatment of GC to enhance anti-tumor immunity.

Disclosure statement

No potential conflict of interest was reported by the author(s).

Funding

Author contributions

Conception and design: J. Su, W.H. Guo, Y.F. Hu. Methodology, data curation, formal analysis, investigation and experiment: J. Su, X.Y. Mao, L.Z. Wang, Z.A. Chen. W.S. Wang, C.Y. Zhao. Statistical analysis, biostatistics, computational analysis: J. Su, W.H. Guo, Y.F. Hu. Writing, review, and/or revision of the manuscript: J. Su, Y.F. Hu. Administrative, technical, or material support: G.X. Li, W.H. Guo, Y.F. Hu. All authors read and approved the final manuscript.

Data availability statement

The datasets generated during and/or analyzed during the current study are available from the corresponding author upon reasonable request.

Ethics statement

This study was approved by the Institutional Ethics Committee of Nanfang Hospital, Southern Medical University, China. The animal experiment in this study was approved by the Animal Care and Use Committee of Southern Medical University and all procedures performed followed the guidance of the Laboratory Animal Center.

ORCID

Yanfeng Hu http://orcid.org/0000-0001-5608-3587

References

1. Ngwa VM, Edwards DN, Philip M, Chen J. Microenvironmental Metabolism Regulates Antitumor Immunity. Cancer Res. 2019;79 (16):4003–4008. doi:10.1158/0008-5472.CAN-19-0617.
2. Chandel NS. Glycolysis. Cold Spring Harb Perspect Biol. 2021;13 (5):a040535. doi:10.1101/cshperspect.a040535.

3. Liberti MV, Locasale JW. The Warburg effect: how does it benefit cancer cells? Trends Biochem Sci. 2016;41(3):211–218. doi:10.1016/j.tibs.2015.12.001.

4. Rabinowitz JD, Enerbäck S. Lactate: the ugly duckling of energy metabolism. Nat Metab. 2020;2(7):566–571. doi:10.1038/s42255-020-0243-4.

5. Certo M, Tsai CH, Pucino V, Ho PC, Mauro C. Lactate modulation of immune responses in inflammatory versus tumour microenvironments. Nat Rev Immunol. 2021;21(3):151–161. doi:10.1038/s41577-020-0406-2.

6. Ippolito L, Morandi A, Giannoni E, Chiarugi P. Lactate: a metabolic driver in the tumour landscape. Trends Biochem Sci. 2019;44(2):153–166. doi:10.1016/j.tibs.2018.10.011.

7. García-Cañaveras JC, Chen L, Rabinowitz JD. The Tumor Metabolic Microenvironment: Lessons from Lactate. Cancer Res. 2019;79(13):3155–3162. doi:10.1158/0008-5472.CAN-18-3726.

8. Xie D, Zhu S, Bai L. Lactic acid in tumor microenvironments causes dysfunction of NKT cells by interfering with mTOR signaling. Sci China Life Sci. 2016;59(12):1290–1296. doi:10.1007/s11427-016-0348-7.

9. Roland CL, Arumugam T, Deng D, Liu SH, Philip B, Gomez S, Burns WR, Ramachandran V, Wang H, Cruz-Monserrate Z. et al. Cell surface lactate receptor GPR81 is crucial for cancer cell survival. Cancer Res. 2014;74(18):5301–5310. doi:10.1158/0008-5472.CAN-14-0319.

10. Zhao Y, Li M, Yao X, Fei Y, Lin Z, Li Z, Cai K, Zhao Y, Luo Z. GPR81/MCT1 regulates tumor ferroptosis through the Lactate-Mediated AMPK-SCD1 activity and its therapeutic implications. Cell Rep. 2020;33(10):108487. doi:10.1016/j.celrep.2020.108487.

11. Kumagai S, Koyama S, Itahashi K, Tanegashima T, Lin YT, Togashi Y, Kamada T, Irie T, Okumura G, Kono H. et al. Lactic acid promotes PD-1 expression in regulatory T cells in highly glycolytic tumor microenvironments. Cancer Cell. 2022;40(2):201–218. doi:10.1016/j.ccell.2022.01.001.

12. Lundø K, Trauelsen M, Pedersen SF, Schwartz TW. Why Warburg Works: lactate controls immune evasion through GPR81. Cell Metab. 2020;31(4):666–668. doi:10.1016/j.cmet.2020.03.001.

13. Sathe A, Grimes SM, Lau BT, Chen J, Suarez C, Huang RJ, Poultsides G, Ji HP. Single-cell genomic characterization reveals the cellular reprogramming of the gastric tumor microenvironment. Clin Cancer Res. 2020;26(11):2640–2653. doi:10.1158/1078-0432.CCR-19-3231.

14. Zheng Y, Chen Z, Han Y, Han L, Zou X, Zhou B, Hu R, Hao J, Bai S, Xiao H. et al. Immune suppressive landscape in the human esophageal squamous cell carcinoma microenvironment. Nat Commun. 2020;11(1):6268. doi:10.1038/s41467-020-20019-0.

15. Su J, Guo W, Chen Z, Wang L, Liu H, Zhao L, Lin T, Li F, Mao X, Huang H. et al. Safety and short-term outcomes of laparoscopic surgery for advanced gastric cancer after neoadjuvant immunotherapy: a retrospective cohort study. Front Immunol. 2022;13:1078196. doi:10.3389/fimmu.2022.1078196.

16. Janjigian YY, Shitara K, Moehler M, Garrido M, Salman P, Shen L, Wyrwicz L, Yamaguchi K, Skoczylas T, Campos Bragagnoli A. et al. First-line nivolumab plus chemotherapy versus chemotherapy alone for advanced gastric, gastro-oesophageal junction, and oesophageal adenocarcinoma (CheckMate 649): a randomised, open-label, phase 3 trial. Lancet. 2021;398(10294):27–40. doi:10.1016/S0140-6736(21)00797-2.

17. Tay C, Tanaka A, Sakaguchi S. Tumor-infiltrating regulatory T cells as targets of cancer immunotherapy. Cancer Cell. 2023;41(3):450–465. doi:10.1016/j.ccell.2023.02.014.

18. Lee JC, Mehdizadeh S, Smith J, Young A, Mufazalov IA, Mowery CT. et al. Regulatory T cell control of systemic immunity and immunotherapy response in liver metastasis. Sci Immunol. 2020;5(52):eaba0759. doi:10.1126/sciimmunol.aba0759.

19. Bessede A, Marabelle A, Guégan JP, Danlos FX, Cousin S, Peyraud F, Chaput N, Spalato M, Roubaud G, Cabart M. et al. Impact of acetaminophen on the efficacy of immunotherapy in cancer patients. Ann Oncol. 2022;33(9):909–915. doi:10.1016/j.annonc.2022.05.010.

20. De Simone M, Arrigoni A, Rossetti G, Gruarin P, Ranzani V, Politano C, Bonnal RP, Provasi E, Sarnicola M, Panzeri I. et al. Transcriptional landscape of human tissue lymphocytes unveils uniqueness of tumor-infiltrating T regulatory cells. Immunity. 2016;45(5):1135–1147. doi:10.1016/j.immuni.2016.10.021.

21. Togashi Y, Shitara K, Nishikawa H. Regulatory T cells in cancer immunosuppression - implications for anticancer therapy. Nat Rev Clin Oncol. 2019;16(6):356–371. doi:10.1038/s41571-019-0175-7.

22. Wang D, Yang L, Yu W, Wu Q, Lian J, Li F, Liu S, Li A, He Z, Liu J. et al. Colorectal cancer cell-derived CCL20 recruits regulatory T cells to promote chemoresistance via FOXO1/CEBPB/NF-κB signaling. J Immunother Cancer. 2019;7(1):215. doi:10.1186/s40425-019-0701-2.

23. Hoelzinger DB, Smith SE, Mirza N, Dominguez AL, Manrique SZ, Lustgarten J. Blockade of CCL1 inhibits T regulatory cell suppressive function enhancing tumor immunity without affecting T effector responses. J Immunol. 2010;184(12):6833–6842. doi:10.4049/jimmunol.0904084.

24. Tan MC, Goedegebuure PS, Belt BA, Flaherty B, Sankpal N, Gillanders WE, Eberlein TJ, Hsieh C-S, Linehan DC. Disruption of CCR5-dependent homing of regulatory T cells inhibits tumor growth in a murine model of pancreatic cancer. J Immunol. 2009;182(3):1746–1755. doi:10.4049/jimmunol.182.3.1746.

25. Gobert M, Treilleux I, Bendriss-Vermare N, Bachelot T, Goddard-Leon S, Arfi V, Biota C, Doffin AC, Durand I, Olive D. et al. Regulatory T cells recruited through CCL22/CCR4 are selectively activated in lymphoid infiltrates surrounding primary breast tumors and lead to an adverse clinical outcome. Cancer Res. 2009;69(5):2000–2009. doi:10.1158/0008-5472.CAN-08-2360.

26. Ji L, Qian W, Gui L, Ji Z, Yin P, Lin GN, Wang Y, Ma B, Gao W-Q. Blockade of β-Catenin–Induced CCL28 suppresses gastric cancer progression via inhibition of Treg cell infiltration. Cancer Res. 2020;80(10):2004–2016. doi:10.1158/0008-5472.CAN-19-3074.

27. Rogers AB, Taylor NS, Whary MT, Stefanich ED, Wang TC, Fox JG. Helicobacter pylori but not high salt induces gastric intraepithelial neoplasia in B6129 mice. Cancer Res. 2005;65(23):10709–10715. doi:10.1158/0008-5472.CAN-05-1846.

28. Liu W, Putnam AL, Xu-Yu Z, Szot GL, Lee MR, Zhu S, Gottlieb PA, Kapranov P, Gingeras TR, de St. Groth BF. et al. CD127 expression inversely correlates with FoxP3 and suppressive function of human CD4+ T reg cells. J Exp Med. 2006;203(7):1701–1711. doi:10.1084/jem.20060772.

29. Marshall LA, Marubayashi S, Jorapur A, Jacobson S, Zibinsky M, Robles O, Hu DX, Jackson JJ, Pookot D, Sanchez J. et al. Tumors establish resistance to immunotherapy by regulating Treg recruitment via CCR4. J Immunother Cancer. 2020;8(2):e000764. doi:10.1136/jitc-2020-000764.

30. Huo S, Luo Y, Deng R, Liu X, Wang J, Wang L, Zhang B, Wang F, Lu J, Li X. et al. EBV-EBNA1 constructs an immunosuppressive microenvironment for nasopharyngeal carcinoma by promoting the chemoattraction of Treg cells. J Immunother Cancer. 2020;8(2):e001588. doi:10.1136/jitc-2020-001588.

31. De La Rochere P, Guil-Luna S, Decaudin D, Azar G, Sidhu SS, Piaggio E. Humanized mice for the study of immuno-oncology. Trends Immunol. 2018;39(9):748–763. doi:10.1016/j.it.2018.07.001.

32. Wang YA, Li XL, Mo YZ, Fan CM, Tang L, Xiong F, Guo C, Xiang B, Zhou M, Ma J. et al. Effects of tumor metabolic microenvironment on regulatory T cells. Mol Cancer. 2018;17(1):168. doi:10.1186/s12943-018-0913-y.

33. Nagase H, Takeoka T, Urakawa S, Morimoto-Okazawa A, Kawashima A, Iwahori K, Takiguchi S, Nishikawa H, Sato E, Sakaguchi S. et al. ICOS+ Foxp3+ TILs in gastric cancer are prognostic markers and effector regulatory T cells associated with Helicobacter pylori. Int J Cancer. 2017;140(3):686–695. doi:10.1002/ijc.30475.

34. Sun S, Li H, Chen J, Qian Q. Lactic acid: No Longer an Inert and end-product of Glycolysis. Physiol (Bethesda). 2017;32(6):453–463. doi:10.1152/physiol.00016.2017.

35. Walenta S, Schroeder T, Mueller-Klieser W. Lactate in solid malignant tumors: potential basis of a metabolic classification in clinical oncology. Curr Med Chem. 2004;11(16):2195–2204. doi:10.2174/0929867043364711.

36. Faubert B, Li KY, Cai L, Hensley CT, Kim J, Zacharias LG, Yang C, Do QN, Doucette S, Burguete D. et al. Lactate Metabolism in Human Lung Tumors. Cell. 2017;171(2):358–371.e9. doi:10.1016/j.cell.2017.09.019.

37. Liu N, Luo J, Kuang D, Xu S, Duan Y, Xia Y, Wei Z, Xie X, Yin B, Chen F. et al. Lactate inhibits ATP6V0d2 expression in tumor-associated macrophages to promote HIF-2α–mediated tumor progression. J Clin Invest. 2019;129(2):631–646. doi:10.1172/JCI123027.

38. Girgis H, Masui O, White NM, Scorilas A, Rotondo F, Seivwright A, Gabril M, Filter ER, Girgis AH, Bjarnason GA. et al. Lactate dehydrogenase A is a potential prognostic marker in clear cell renal cell carcinoma. Mol Cancer. 2014;13(1):101. doi:10.1186/1476-4598-13-101.

39. Brand A, Singer K, Koehl GE, Kolitzus M, Schoenhammer G, Thiel A, Matos C, Bruss C, Klobuch S, Peter K. et al. LDHA-Associated lactic acid production blunts tumor immunosurveillance by T and NK Cells. Cell Metab. 2016;24(5):657–671. doi:10.1016/j.cmet.2016.08.011.

40. Hong CS, Graham NA, Gu W, Espindola Camacho C, Mah V, Maresh EL, Alavi M, Bagryanova L, Krotee PAL, Gardner BK. et al. MCT1 modulates cancer cell pyruvate export and growth of tumors that Co-express MCT1 and MCT4. Cell Rep. 2016;14(7):1590–1601. doi:10.1016/j.celrep.2016.01.057.

41. Polański R, Hodgkinson CL, Fusi A, Nonaka D, Priest L, Kelly P, Trapani F, Bishop PW, White A, Critchlow SE. et al. Activity of the monocarboxylate transporter 1 inhibitor AZD3965 in small cell lung cancer. Clin Cancer Res. 2014;20(4):926–937. doi:10.1158/1078-0432.CCR-13-2270.

42. Brown TP, Bhattacharjee P, Ramachandran S, Sivaprakasam S, Ristic B, Sikder MOF, Ganapathy V. The lactate receptor GPR81 promotes breast cancer growth via a paracrine mechanism involving antigen-presenting cells in the tumor microenvironment. Oncogene. 2020;39(16):3292–3304. doi:10.1038/s41388-020-1216-5.

43. Yang X, Lu Y, Hang J, Zhang J, Zhang T, Huo Y, Liu J, Lai S, Luo D, Wang L. et al. Lactate-modulated immunosuppression of myeloid-derived suppressor cells contributes to the radioresistance of pancreatic cancer. Cancer Immunol Res. 2020;8(11):1440–1451. doi:10.1158/2326-6066.CIR-20-0111.

44. Feng J, Yang H, Zhang Y, Wei H, Zhu Z, Zhu B, Yang M, Cao W, Wang L, Wu Z. et al. Tumor cell-derived lactate induces TAZ-dependent upregulation of PD-L1 through GPR81 in human lung cancer cells. Oncogene. 2017;36(42):5829–5839. doi:10.1038/onc.2017.188.

45. Nishikawa H, Koyama S. Mechanisms of regulatory T cell infiltration in tumors: implications for innovative immune precision therapies. J Immunother Cancer. 2021;9(7):e002591. doi:10.1136/jitc-2021-002591.

46. Gajewski TF, Corrales L, Williams J, Horton B, Sivan A, Spranger S. Cancer immunotherapy targets based on understanding the T Cell-Inflamed versus Non-T Cell-Inflamed tumor Microenvironment. Adv Exp Med Biol. 2017;1036:19–31. doi:10.1007/978-3-319-67577-0_2

47. Kumagai S, Koyama S, Nishikawa H. Antitumour immunity regulated by aberrant ERBB family signalling. Nat Rev Cancer. 2021;21(3):181–197. doi:10.1038/s41568-020-00322-0.

48. Serrels A, Lund T, Serrels B, Byron A, McPherson RC, von Kriegsheim A, Gómez-Cuadrado L, Canel M, Muir M, Ring J. et al. Nuclear FAK controls chemokine transcription, tregs, and evasion of anti-tumor immunity. Cell. 2015;163(1):160–173. doi:10.1016/j.cell.2015.09.001.

49. Isse K, Harada K, Zen Y, Kamihira T, Shimoda S, Harada M, Nakanuma Y. Fractalkine and CX3CR1 are involved in the recruitment of intraepithelial lymphocytes of intrahepatic bile ducts. Hepatology. 2005;41(3):506–516. doi:10.1002/hep.20582.

50. Lee S, Latha K, Manyam G, Yang Y, Rao A, Rao G. Role of CX3CR1 signaling in malignant transformation of gliomas. Neuro Oncol. 2020;22(10):1463–1473. doi:10.1093/neuonc/noaa075.

51. Yu SJ, Ma C, Heinrich B, Brown ZJ, Sandhu M, Zhang Q, Fu Q, Agdashian D, Rosato U, Korangy F. et al. Targeting the crosstalk between cytokine-induced killer cells and myeloid-derived suppressor cells in hepatocellular carcinoma. J Hepatol. 2019;70(3):449–457. doi:10.1016/j.jhep.2018.10.040.

52. Chen EB, Zhou ZJ, Xiao K, Zhu GQ, Yang Y, Wang B, Zhou S-L, Chen Q, Yin D, Wang Z. et al. The miR-561-5p/CX3CL1 Signaling Axis Regulates Pulmonary Metastasis in Hepatocellular Carcinoma Involving CX3CR1+ Natural Killer Cells Infiltration. Theranostics. 2019;9(16):4779–4794. doi:10.7150/thno.32543.

53. Baldwin AS. Regulation of cell death and autophagy by IKK and NF-κB: critical mechanisms in immune function and cancer. Immunol Rev. 2012;246(1):327–345. doi:10.1111/j.1600-065X.2012.01095.x.

54. Peng C, Ouyang Y, Lu N, Li N. The NF-κB signaling pathway, the microbiota, and Gastrointestinal Tumorigenesis: recent advances. Front Immunol. 2020;11:1387. doi:10.3389/fimmu.2020.01387.

55. Nagumo Y, Kandori S, Tanuma K, Nitta S, Chihara I, Shiga M, Hoshi A, Negoro H, Kojima T, Mathis BJ. et al. PLD1 promotes tumor invasion by regulation of MMP-13 expression via NF-κB signaling in bladder cancer. Cancer Lett. 2021;511:15–25. doi:10.1016/j.canlet.2021.04.014.

56. Lu W, Zhang G, Zhang R, Flores LG, Huang Q, Gelovani JG, Li C. Tumor site–specific silencing of NF-κB p65 by targeted hollow gold nanosphere–mediated photothermal transfection. Cancer Research. 2010;70(8):3177–3188. doi:10.1158/0008-5472.CAN-09-3379.